DISCLAIMER

MAR 2 5 1991

Seismic Fragility Evaluation of Unreinforced Masonry Walls

Y.J. Park, C.H. Hofmayer, M. Reich
Brookhaven National Laboratory
Upton, NY USA

S.K. Lee
Korea Institute of Nuclear Safety
Taejon, Korea

MASTER

ABSTRACT

A practical analysis scheme to evaluate the seismic fragility of unreinforced masonry walls which are used at various places in older reactor facilities is presented. Among the several failure modes for such walls, the out-of-plane bending failure is considered to be a major risk contributor in seismic PRA studies. In order to evaluate this failure mode, the use of an equivalent linear approximation method is examined based on comparisons with available test data and nonlinear time history analyses.

1 INTRODUCTION

Past seismic PRA studies of nuclear facilities indicate that unreinforced masonry walls can be weak-links due to low seismic resistance against in-plane shear and out-of-plane bending actions. These two failure modes require distinctively different analytical approaches due to the different inelastic behavior near the failure region.

For the in-plane shear failure, due to the low ductility, the seismic capacity is determined directly from the median shear stress, v_u, such as the following equation which is based on available test data (e.g., Hidalgo and Luders, 1986);

$$v_u = 2/3 \ (4-M/Vd)\sqrt{f'_m} + 0.1 \ \sigma_o \qquad (1)$$

where, M/Vd is the shear span ratio, f'_m is the compressive strength of masonry and σ_o is the average axial stress. For the case of infilled masonry walls, a certain ductility can be considered due to the additional confinement by the surrounding frame (e.g., de Beek et al. 1984).

For the out-of-plane bending failure, on the other hand, a nonlinear dynamic analysis may be required due to early cracking (or existing cracking) and subsequent rigid-body rocking motion. For this purpose, a practical analytical approach is described here based on a conservative linear approximation of structural responses.

2 EQUIVALENT LINEAR MODEL (RESERVE ENERGY METHOD)

To avoid time consuming numerical time history analyses, an alternative approach to practically handle the above problem is considered by using a SDOF

system with an equivalent linear property (e.g., Wesley et al. 1980). In thismethod, the cracking strength of the masonry wall is neglected, and an idealized rigid-body motion is assumed as illustrated in Figure 1. The wall is subjected to an out-of-plane bending due to the inertia force and a forced displacement, u_f, at the top, which may be regarded as the interstory deformation when the wall is located between two stories of a building. The failure of the wall is identified by the following criteria:

$$u \geq t - 0.5 \ u_f \qquad\qquad (2)$$

in which, u, is the deformation at the mid-height of the wall and t is the wall thickness. When the above rigid-body motion is represented by a SDOF system, the effective weight, W_e, is given by

$$W_e - 1/3 \ W_t \qquad\qquad (3)$$

in which W_t, is the total weight of the wall. The rocking motion strength, F_m, is calculated using the notation of Figure 1. The axial force is assumed to be applied at the edge of the block walls.

$$F_m - F_1 + F_2 - (4N + 2 \ W_t) \ t/\ell \qquad\qquad (4)$$

   The restoring force characteristics of a masonry wall under out-of-plane bending is shown in Figure 2(a). After the strength drop due to cracking, the restoring force possesses a negative stiffness due to the P-δ effect. This peculiar nonlinear characteristic associated with unreinforced masonry walls under out-of-plane bending has been clearly demonstrated in dynamic failure tests of adobe walls (Bariola and Sozen, 1990). According to the reserve energy method (Wesley et al., 1980), this nonlinear restoring force behavior is represented by a linear system with an equal potential energy. In this scheme, the failure is identified when the linear response exceeds the wall thickness, t, as illustrated in Figure 2(b). Therefore, the stiffness of the equivalent linear system is given by,

$$K_e - F_m/t \qquad\qquad (5)$$

3 COMPARISON WITH DYNAMIC TEST RESULTS

The foregoing approach is compared against available test results of unreinforced concrete block walls by Agbabian, et al., 1981. Ten (10) unreinforced concrete block walls were tested under out-of-plane bending excitation applied by two actuators at the bottom and the top. As the excitation motions, either a recorded ground motion or the floor response of a typical reinforced concrete building were used. The excitation level was gradually increased until failure.
   The prism compressive strength of the concrete blocks are as follows:

six inch walls: $f'_m - 2432$ psi
eight inch walls: $f'_m - 2493$ psi

   Table 1 lists the comparison of wall collapse strength in terms of the ratio of the spectral velocity. Therefore, these values represent the safety factor associated with the foregoing equivalent linear modeling. The ratio is given by a range since the excitation corresponding to the wall collapse cannot be

determined precisely. The listed average ratio was obtained by taking average ratios corresponding to the test run during which the wall collapsed and the run right before it. Using these average ratio values, the median safety factor is calculated to be 1.02 with a C.O.V. of 0.14. It seems that the equivalent linear model reasonably predicts the wall collapse strength. It should be noted that during the tests the earthquake excitations were applied to a wall many times until a wall reached failure. This would lower the strength of the walls due to cracking and the strength deterioration in mortar. Therefore, the foregoing analysis method is expected to give a more conservative estimate of the seismic fragility when a block wall is subjected to a single seismic motion.

4 COMPARISON WITH NUMERICAL ANALYSIS

To further evaluate the seismic strength of unreinforced masonry walls under out-of-plane bending and the accuracy of the foregoing approximate linear modeling, numerical integration analyses were performed for typical concrete block walls. The following properties are assumed for all the wall models:

Wall Thickness:	$t = 5.63''$
Wall Height:	$\ell = 10'$
Prism compressive Strength:	$f'_m = 2.5$ ksi
Modulus of Elasticity:	$E = 1000 f'_m = 2500$ ksi
Unit Weight:	140 lbs/ft^3
Boundary Condition:	Fixed at base, pin-connected at top

Four levels of constant axial stress are considered, i.e., 0, 1, 2 and 5 percent of the prism compressive strength of concrete blocks. As the input motion, the following six accelerograms are used.

Name	Event	Peak Velocity (in/sec)
Castaic, N21E	San Fernando, 1971	23
El Centro, N00E	Imperial Valley, 1979	13
Pacoima, S16E	San Fernando, 1971	46
Parkfield, N65W	Parkfield, 1966	19
Hachinohe	Tokachi-Oki, Japan 1968	15
Reg Guide 1.60	Generated Motion	54

The structural damping was assumed to be 1% for the nonlinear models (Bariola, et al., 1990) and 7% for the linear models. The results of the time history analysis are tabulated in Table 2. Based on these results, the existence of axial forces seems to significantly enhance the seismic capacity of unreinforced walls under out-of-plane bending. The linear approximation generally gives a conservative estimate of seismic capacity when compared with nonlinear analyses. Considering the fact that the nonlinear analyses do not consider the strength deterioration, which may have been a significant factor in the foregoing dynamics tests, the observed conservativeness may be consistent with the previous comparison with test data.

5 EFFECT OF ARCHING ACTION

An additional conservatism exists in the foregoing analyses since the rotational restraints at the boundaries are neglected. The rotational

restraint due to the wall's horizontal displacement induces an arching mechanism. This arching mechanism is illustrated in Figure 3, in which the additional resistance by the arch action is represented by the horizontal force at the mid-height, F_a, and the restraint from the support structure, e.g., RC floor beams and slabs, is represented by an elastic spring, K_s. The rotational deformation, θ, shown in Figure 3, is related to the horizontal displacement at the mid-height, u,

$$\theta = 2u/\ell \tag{6}$$

The vertical force induced by the arching action, Q, is expressed as,

$$Q = \frac{C_k}{(1+C_k)} \cdot \frac{4EAt}{\ell^2} \cdot u \tag{7}$$

in which, EA/ℓ represents the axial stiffness of the block wall; and C_k is the ratio of the stiffness, K_s, to the walls stiffness, EA/ℓ. Considering the equilibrium of the block wall during rotation, the horizontal resistance, F_a, is expressed by a nonlinear function of the horizontal displacement, u.

$$F_a = \frac{16C_k EAt}{(1+C_k)\ell^3} (ut - u^2) \tag{8}$$

The above additional resistance force is superposed on the restoring force of Figure 2; a typical result is shown in Figure 4. Using the same rule as in the foregoing energy reserve method, a linear model with equal potential energy is determined as illustrated in Figure 4. The stiffness of the linear model is obtained as,

$$K_e = \frac{1}{\ell} \left\{ 4N + 2W_t + \frac{16C_k EAt^2}{3(1 + C_k)\ell^2} \right\} \tag{9}$$

The results of time history analyses are tabulated in Table 3 in terms of the peak base motion velocity corresponding to the wall collapse for Castaic 1971 and El Centro 1979. The results indicate that arching action increases the seismic capacity significantly. When the stiffness of the restraint is 10% of the axial stiffness of the block wall, the seismic capacity of walls under out-of-plane bending increases to the extent that such a failure mode would not be expected to occur when compared with other failure modes, e.g., the in-plane shear failure mode. The linear approximation seems to produce a reasonable prediction when the stiffness has a high value, although the predicted values are not always on the conservative side, for walls with different thickness.

REFERENCES

Adham, S.A., and Agbabian, M.S., "Seismic Design Guidelines for Tilt-up-Wall Buildings Based on Experimental and Analytical Models," 3rd U.S. National Conference on Earthquake Engineering, Charleston, SC, 1986.

Agbabian et al., "Methodology for Mitigation of Seismic Hazards in Existing Unreinforced Masonry Buildings," ABK, El Segundo, CA, August 1981.

Bariola, J., and Sozen, M.A., "Seismic Tests of Adobe Walls," Earthquake Spectra, Vol. 6, No. 1, 1990, pp. 37-56.

de Beeck, M.S., and Bartolome, A.S., "Relevant Masonry Projects Carried Out in the Structures Laboratory at the Catholic University of Peru," 8th WCEE, San Francisco, CA, July 1984, Vol. VI, pp. 823-830.

Hidalgo, P., and Luders, C., "Shear Strength of Reinforced Masonry Walls under Earthquake Excitation," 3rd National Conference on Earthquake Engineering, Charleston, SC, August 1986.

Wesley, D.A., Kennedy, R.P., and Richter, P.J., "Analysis of the Seismic Collapse of Unreinforced Masonry Wall Structures," 7th WCEE, Istanbul, Turkey, 1980, pp. 411-418.

TABLE 1 Properties of Tested Walls and Comparison with Analysis

Specimen Number	H (ft)	Th (in)	W_e (kips)	F_m (kips)	Frequency (Hz)	Spectral Ratio S_v(test)/S_v(cal)	Average Ratio
5	10	5.63	1.15	1.64	1.56	0.80 - 0.98	0.89
6	10	5.63	1.15	0.58	0.93	0.77 - 1.28	1.03
10	16	7.63	1.30	0.53	0.74	0.64 - 1.17	0.91
11	16	7.63	1.30	0.86	0.93	0.91 - 0.92	0.92
13	10	7.63	0.79	0.66	1.03	0.88 - 1.06	0.97
14	10	7.63	0.79	0.66	1.03	1.06 - 1.06	1.06
15	10	7.63	0.79	1.19	1.39	0.83 - 0.92	0.88
16	10	5.63	0.62	0.43	1.12	1.13 - 1.28	1.21
17	10	5.63	0.62	0.43	1.12	1.28 - 1.36	1.32
18	10	5.63	0.62	0.82	1.52	1.00 - 1.11	1.06

TABLE 2 Comparison of Nonlinear and Linear Analyses

Wall Thickness	Axial Stress	Peak Ground Motion Velocity at Failure (in/sec)						
		Castaic	Pacoima	Hachi-nohe	El-centro	Park-field	Reg. 1.60	Average
6 in	0%	16.2	16.3	17.0	13.1	21.3	16.2	16.7
		(9.6)	(6.3)	(6.7)	(5.1)	(8.2)	(6.3)	(7.0)
	1%	27.5	57.4	56.8	22.2	35.5	46.4	41.0
		(16.5)	(40.4)	(21.9)	(10.5)	(38.7)	(17.9)	(24.3)
	2%	39.3	74.6	114.7	30.7	53.3	67.3	63.3
		(18.5)	(28.8)	(54.0)	(14.5)	(20.5)	(26.0)	(27.1)
	5%	79.4	160.6	286.3	70.7	110.6	163.2	145.1
		(37.4)	(75.7)	(134.9)	(40.7)	(42.7)	(62.9)	(65.7)

* Values in ( ) are by linear model approximation

TABLE 3 Effect of Arching Action

Wall Thickness	Axial Stress	Peak Velocity at Failure (in/sec) Stiffness Ratio, C_k							
		Castaic				Elcentro			
		0%	0.1%	1%	10%	0%	0.1%	1%	10%
6 in	0%	16.2	20.4	30.9	292.5	13.1	20.7	40.8	254.0
		(9.6)	(9.6)	(18.6)	(205.9)	(5.1)	(9.8)	(20.1)	(146.3)
	1%	27.5	26.8	37.6	295.1	22.2	22.3	41.8	228.1
		(16.5)	(12.6)	(21.7)	(207.7)	(10.5)	(12.8)	(29.4)	(160.6)
	2%	39.3	45.9	63.4	297.1	30.7	33.0	57.4	242.8
		(18.5)	(21.6)	(36.5)	(209.1)	(14.5)	(15.6)	(40.4)	(170.9)
	5%	79.4	84.3	104.7	266.9	70.7	84.1	85.6	280.3
		(37.4)	(39.7)	(49.3)	(229.6)	(40.7)	(39.6)	(53.7)	(197.3)

* Values in ( ) are by linear model approximation

(a)   (b)
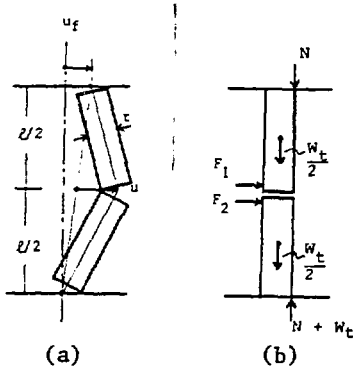
Figure 1 Block Wall Model.
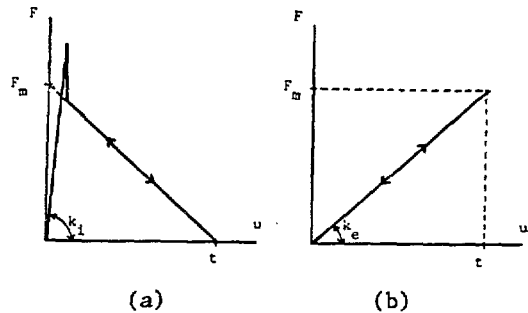

(a)   (b)
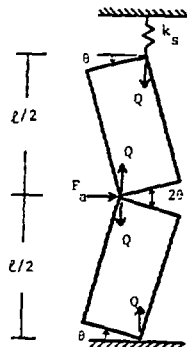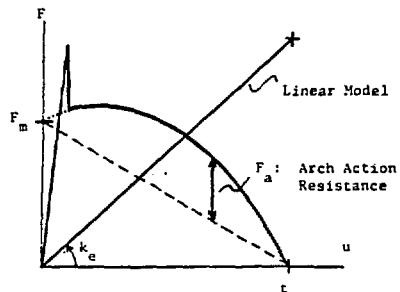
Figure 2 Restoring Force of Block Wall

Figure 3 Arching Action

Figure 4 Restoring Force with Arching Action